J. Magn. Soc. Jpn., **40**, 148-152 (2016)

<Paper>

The Role of B_x Magnetic Field in Reducing B_y Magnetic Noise in Separate Shell Magnetic Shield

A. Mahgoub[1], and I. Sasada[2]

[1] Cairo University, Electrical power and machines, Giza, *12613, Egypt*

[2] Kyushu University, Applied science for electronics and materials, *6-1 Kasuga-koen, Kasuga-shi, Fukuoka 816-8580, Japan*

A new method employing x-axis (horizontal) compensation system is introduced to reduce the magnetic noise measured in y-axis (vertical) in a separate shell magnetic shield. Due to the construction of the separate shell magnetic shield the x-axis incident magnetic field is redistributed generating a y-axis components affecting the operation of the sensors used in MCG measurements. The new method utilizes an active compensation system in x-direction to reduce both the gradient of magnetic field in y-direction and time varying magnetic noise generated in y-axis due to x-axis magnetic fields. Finally, a practical implementation of the adopted active compensation scheme is presented in order to reduce the cross effect from x-axis magnetic fields on y-axis.

Key words: magnetic shielding, Active compensation, MCG, Fluxgates

1. Introduction

Magnetocardiography is a powerful non-invasive tool to detect tiny magnetic field produced from the human heart [1-2]. Yet measuring such small magnetic fields is challenging, since the signals to be measured is three orders of magnitude less than the environmental magnetic fields. Hence a strong magnetic shield is required to provide a magnetically quiet environment for the measurement process [3-5].

Although conventional magnetic shields can provide a high shielding efficiency, they are not widely used as they consist of many layers of high permeable magnetic materials that increase their cost and weight. Active compensation aided with separable magnetic shells is an effective method to mitigate the drawbacks of conventional magnetic shields [6].

Full size separate shell magnetic shield aided with active compensation system in both x-axis and y-axis was introduced [7, 8 and 9]. The shielding system may contain 3 active shielding coils pair for each axis (x-, y-, and z- axes). However, as shown in Fig.1 only one active shielding system will be used in this paper 'i.e. x- axis'. In order to measure the signal from the human heart, the system is prepared such that it can utilize either a matrix of 8*8 fluxgate gradiometers placed in y-axis or SQUID sensor measuring change in y-axis magnetic. The shielding performance of the shield was investigated in [7]. A shielding factor up to 100 and 1000 in x-axis and y-axis respectively at 60 Hz were reported. But the noise level at 1 Hz was not reduced below 100 pT/√Hz for both x-axis and y-axis. Also many line spectra were not completely eliminated at higher frequencies. In order to improve shielding efficiency of the shield, two independent controllers for time varying and static magnetic fields was introduced in [8] to compensate magnetic noise in vertical direction. The noise level was then improved to 30 pT/√Hz at 1 Hz and 3 pT/√Hz noise floor was achieved at higher frequencies. In addition, the effect of x-axis magnetic field on y-axis magnetic field (cross interference) was reported. A method to reduce magnetic field gradient produced in y-axis by overcompensating x-axis magnetic field was proposed earlier; but yet not experimentally verified [9].

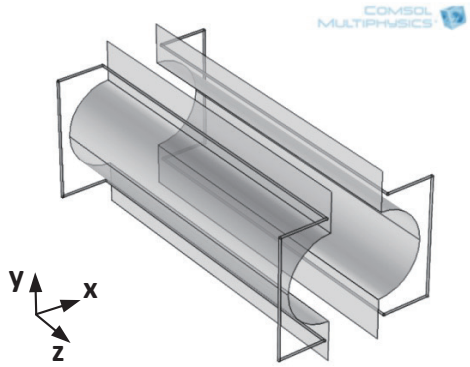

Fig. 1 large-scale separate shell magnetic shield with active compensation coils in x- axis and y- axis. The values are in cm

In this paper, the effect of x-axis magnetic field on y-axis magnetic field is presented. Overcompensation technique is experimentally verified. Moreover, an x-axis active compensation is realized to reduce the effect of time varying components of x-axis on y-axis magnetic fields.

2. FEM validation for overcompensation technique

To demonstrate cross interference between x-axis magnetic field and y-axis magnetic field, a simulation is conducted using the finite element methods (FEM) in the two-dimensional stationary condition. The shielding system consists of three parts; the outermost part is made of magnetic material having a relative permeability of 10000, the middle part and the innermost parts are made of magnetic material having a relative permeability of 40000, and the last one is the

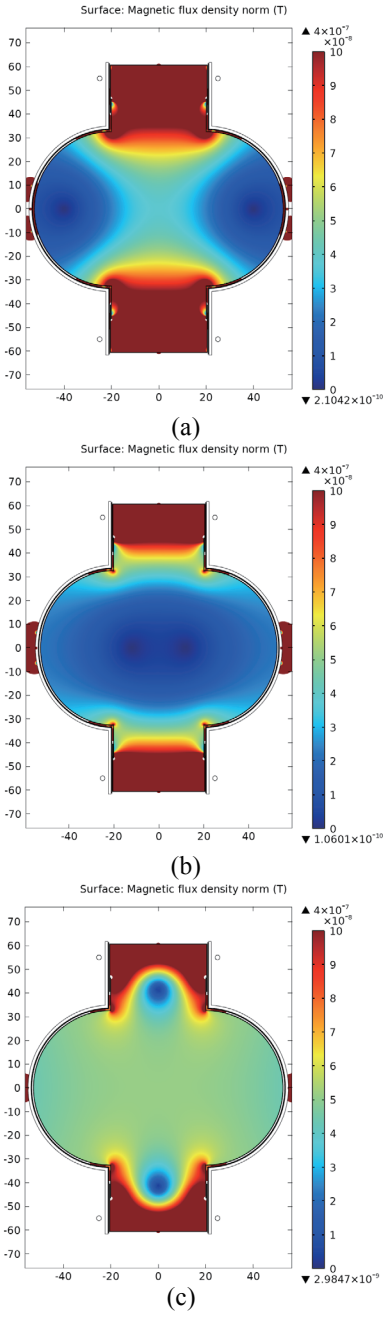

Fig. 2 surface plot of magnetic field distribution inside the shield for three cases (a) low level of compensation (b) optimum level of compensation (c) overcompensation. All axes are in cm.

magnetic bridges linking the shell parts which are made of the same magnetic material of 40000 relative permeability. The compensation coils used in the simulation are single turn coil as shown in Fig. 1.

An external magnetic field of 10 μT is imposed to the shielding system in positive x-axis. Different active compensation currents are injected into compensation system to compensate external magnetic field and magnetic field in y-axis is then calculated.

As described in [9], a surface plot of magnetic field distribution inside the shield can be calculated. As the coils used for active compensation are concentric coils; the fields produced from these coils are not uniform. So at low level of compensation ($B_{active} < B_{external}$) the null points (points with minimum magnetic flux density) occur at the center of the coils. But if the level of compensation increases, the magnetic flux lines become denser, and the uniformity increases. Hence, further increase in the level of compensation will lead to decreasing the gradient of the magnetic field inside the shield. But the problem is that the null points move upward, and the magnetic field at the area of interest become overcompensated ($B_{active} > B_{external}$) and reverse its direction. It should be noted that in Fig. 2, excessive overcompensation current is used to show overcompensation effect for the sake of figure clarity and readability.

The effect of overcompensation in y-axis magnetic field may then be explained by the fact that around the point of minimum or maximum a very high gradient exists. In addition, between two consecutive minimum points or maximum points it shall exist a point with zero gradient. As a result, when the null points move to y-axis as depicted in Fig. 2c, a point with zero/minimum gradient may exist in this direction [9].

So in order to determine the optimum overcompensation current to be injected in x-axis compensation system, active compensation current is increased gradually and the magnetic field inside the shield is calculated. The difference between the reading of two points, in the center of the shield relative to z- axis, separated by 5cm is calculated at x = 10 cm and x = 5 cm to cover at least 20 cm width covering all the area of measurements; i.e. chest area (5 cm in y-axis is selected to fit for gradiometer sensor base line. In case of using a sensor with different base line, this value should be modified). Also the value of the B_x component at the same position is calculated as shown in Fig. 3, 4.

According to Fig. 3, injecting a current of 7.5 A in the active compensation coil cancels the external magnetic flux component in x- axis. However, the gradient of y-component magnetic flux density is not zero and it increases as the distance of measuring point from the center increases in x-axis as shown in Fig. 4. Increasing the current of active compensation coil to nearly 7.7 A will cause the x- component of magnetic flux density to be overcompensated. Despite that, the gradient of magnetic flux density in y-axis is canceled completely as illustrated in Fig. 4.

It worth mentioning that excessive overcompensation of x- axis magnetic flux density may seem not to affect main gradiometers/sensors directly, but small unavoidable vibrations of gradiometers/sensors may arise the effect of this component on the measured magnetic field. In addition, increasing the overcompensation will cause the gradient itself to increase, turning active compensation coils to be the source of noise as depicted in Fig. 4. As a consequence, the overcompensation current should be tightly kept

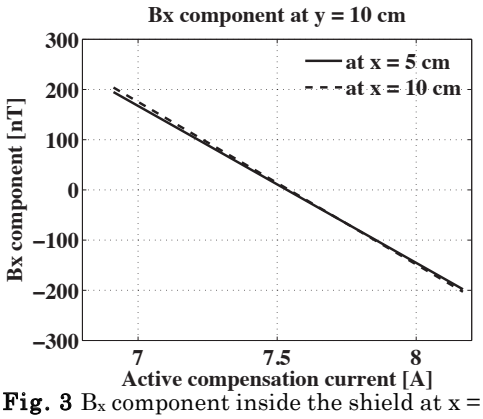

Fig. 3 B_x component inside the shield at x = 10 cm and x = 5 cm with different active compensation currents.

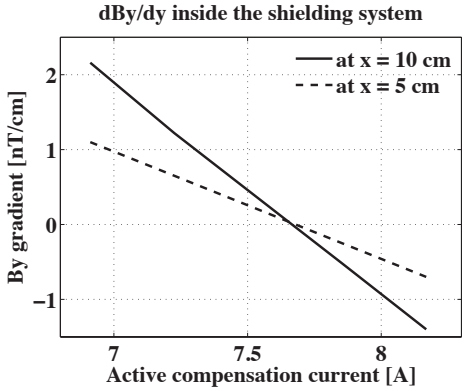

Fig. 4 Magnetic field gradient of B_y component inside the shield at different active compensation level

constant at the the value achieving zero gradient of magnetic flux density component in y-axis at the area of interest [9].

3. Experimental setup

A full size separate shell magnetic shield, described in [7] in details, is used. The system is aided with active shielding system for x- axis magnetic field. The active shielding in x- axis consists of two sets of coils. One coil (A1-A2) is prepared to achieve overcompensation technique and to remove static components. For simplicity this coil is connected to a controlled DC source. The other coil (B1-B2) is prepared to perform the active compensation for time varying components (i.e. connected to the power amplifier output as depicted in Fig. 5). The two sets of coils are grounded with the same ground. Each set of coils consists of one pair of coils; one coil at the right and another one at the left of the shield; see Fig. 5. A proportional - integral (PI) controller controls the second set of coils through the power amplifier. The controller measures the leakage magnetic field using orthogonal Fluxgate (FG) sensor with sensitivity of 0.27 V/μT and bandwidth of 700 Hz [10]. Another two FG sensors are used. One to characterize the magnetic field inside the shield in y-axis and the other one in x-axis to measure the level of compensation. The additional FGs

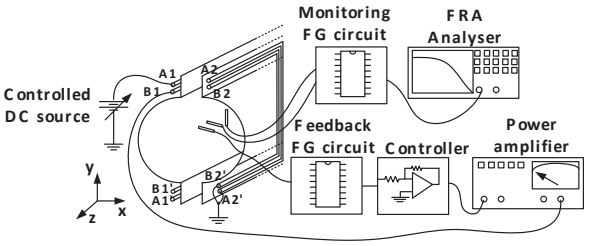

Fig. 5 Schematic diagram showing all components of the active compensation and testing equipment. A1, and A2 are over-compensation coils connected in series. B1, and B2 are active compensation coils connected in series.

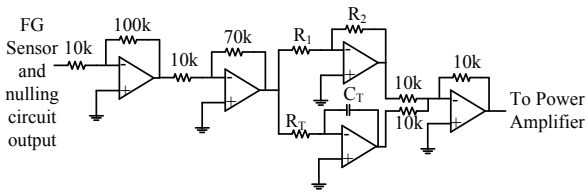

Fig. 6 Controller schematic describing the preamplifier stage and PI controller stage

are connected to Frequency Response analyzer (FRA) as depicted in Fig.5. Feedback sensor is separated by 2 cm in z-direction from the characterizing sensors. The characterization sensors are placed at the center point of the shield.

The PI controller circuit shown in Fig. 6 consists of three stages. The first stage is the nulling circuit to compensate the dc offset inherent the output of FG sensor [10]. The second stage is a two steps preamplifier with total gain of 70. The third stage is the PI controller. The proportional and the integral parts are adjustable. The integral part is set to have a gain of $K_i = 1/(C_T R_T) = 1000\ \text{sec}^{-1}$. The proportional part ($K_p = R_2/R_1$) is ranging from 1 to 10. All control parameters are determined experimentally such that the maximum possible gain is introduced without driving the active compensation current into oscillation.

4. Overcompensation technique validation

The block diagram in Fig. 7 describes the normal compensation condition. It is clear that this system will keep the magnetic field inside the shield to be zero or minimum as much as possible but on the other hand it will not enable us to achieve overcompensation. In order to overcompensate the x-component of the magnetic field, the modified block diagram in Fig. 8 can be adopted. A controlled offset can be added to the output of the flux gate using any adder (summer) circuit before the controller. Hence the controller will increase the control action in order to suppress the excess error seen at its input.

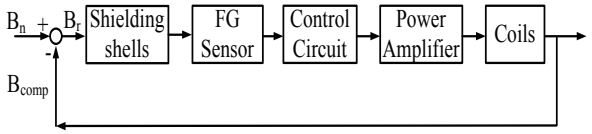

Fig. 7 A block diagram of the active shielding system

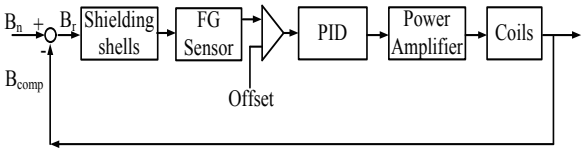

Fig. 8 A block diagram of the active shielding system with modified controller.

Fig. 9 shows the resultant magnetic field inside the shield for four cases: No compensation, under compensation, optimum compensation, and overcompensation. The magnetic field is measured using a fluxgate sensor placed at x = 1.5, 4.5, 7.5 cm vertically. The results show that the magnetic field gradient inside the shield is very much reduced if the magnetic field in x-direction is overcompensated. The ratio between excess current injected and the current needed to fully compensate magnetic field at the center of the shield (optimum compensation) in this case is only 0.057. The magnetic field inside the shield is maintained at 60 nT, improving the resultant magnetic field gradient inside the shield. The gradient drops to less than 1 nT/cm instead of 58 nT/cm when no compensation is used. The gradient is calculated by measuring magnetic flux density at x = 7.5 cm (point with largest magnetic flux density as shown in Fig. 9) divided by the distance from the center line of the shield (i.e. 6 cm).

5. Active compensation in x-axis

In this experiment two sets of coils will be used. One is used for compensating static magnetic field. The second is for compensating the time varying magnetic fields. The static fields will be compensated using DC power supply as stated earlier; see fig. 5. In case of

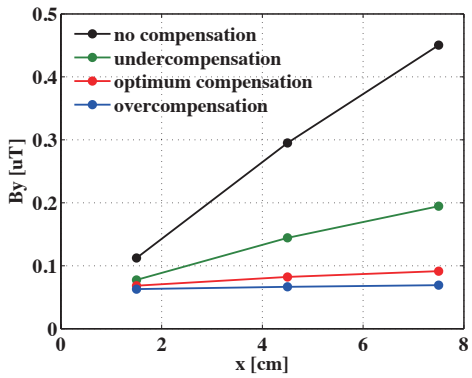

Fig. 9 Distribution of B_y component of magnetic field inside the shield for four cases: no compensation, under compensation, optimum compensation, and overcompensation

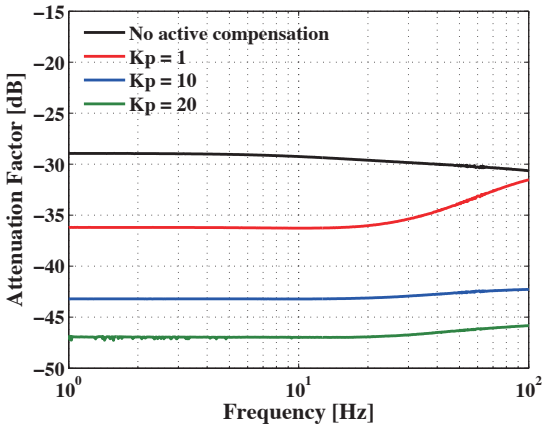

Fig. 10 Frequency response of the attenuation factor of the shield in x-axis at different proportional controller values. The curves are center of the shield.

compensating time varying component, the gain of the controller will be adjusted such that the maximum shielding efficiency is achieved without driving the system into oscillation.

To adjust the gain controller, the value of the proportional controller is changed in steps k_P = 2, 10, and 20. The frequency response at each step was measured as shown in Fig. 10. It is noticed that as the controller gain increases, the shielding factor increases. The maximum shielding factor obtained at low frequency (near 1 Hz) is -47.5 dB, equivalent to 237.13, that is obtained at k_P = 20, that improves from -29 dB, equivalent to 28.1, at no compensation. Further increase in the proportional controller gain leads to oscillation in the system and high current is absorbed from the power amplifier.

Furthermore, the effect of active compensation in x-axis on y-axis magnetic field is investigated. The frequency response of the shield in y-axis is measured using frequency response analyzer for two cases: for the case of no active compensation is used in x-axis and for the case of x-axis compensation system is turned on at the maximum possible gain, k_P = 20. Figure 11 shows the relative position between x-axis fluxgate feedback sensor used for active compensation and y-axis fluxgate sensor used for evaluation. Due to symmetrical configuration of the shielding system the magnetic field at the center line of the shield will be zero, hence the vertical evaluation sensor should be placed off the center. At this point the definition of cross attenuation factor should be introduced. It can be defined as the ratio between the measured magnetic flux density in y-axis and the applied magnetic flux density in x-axis (from disturbing coil). Fig. 12 shows the cross attenuation factor of the vertical component of magnetic flux density due to active compensation in horizontal axis. The result shows that y-axis magnetic field generated due to x-axis magnetic field is attenuated in case of using active compensation. The generated noise in y-axis due to

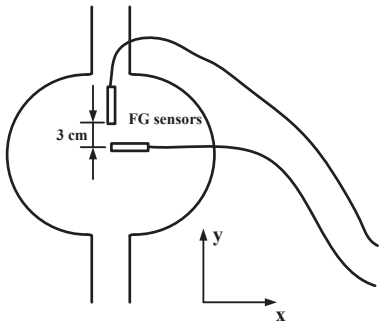

Fig. 11 Schematic showing the relative position between horizontal feedback sensor and vertical evaluation sensor

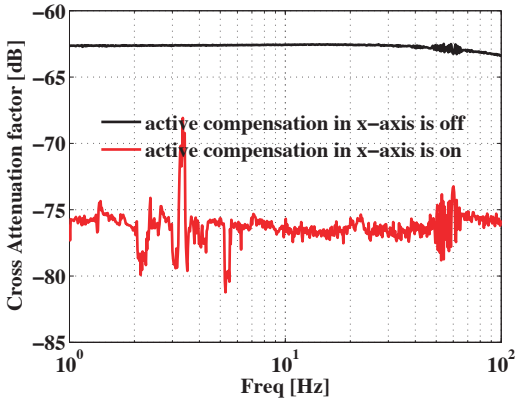

Fig. 12 Frequency response of the attenuation factor of the shield in y-axis at two cases: no x-axis compensation and with active compensation on. The curves are center of the shield.

x-axis magnetic field is reduced by a factor of -75 dB, equivalent to 5623.5, instead of -62.5 dB, equivalent to 1333.52, in case of no active compensation is used. It should be noted that this high shielding factor is not uniform all over the frequency spectrum of interest as shown by the red curve in Fig. 12. This curve indicates how each frequency in y-axis is attenuated after using x-axis active compensation is activated. The fact that all line spectra are not attenuated equally gives a logical indication that not all the measured magnetic noise in y-axis are originated due to external x-axis magnetic field. Hence, x-axis active compensation will not be equally effective on each line spectrum appearing in y-axis measurement and it is needed to combine other y-axis active shielding techniques to the x-axis active compensation in order to remove the remaining magnetic noise inside the shield.

6. Conclusions

Effectiveness of overcompensation technique in reducing magnetic field gradients generated in y-axis magnetic fields is presented. With slightly overcompensating x-axis magnetic field, y-axis gradient is reduced to 1 nT/cm from 58 nT/cm when no compensation is used. For the case of active compensation of time varying magnetic field in x-axis, the shielding factor of noise generated in y-axis is improved from 1333 to 5623.

References

1) Wilfried Andra and Hannes Nowak, *Magnetism in Medicine*, (2007).
2) Macfariane, Peter W.; Oosterom, Adriaan an; Pahlm, Olie; kigfield, Paul; Janse, Michiel; Camm, John, *Comperhensive Electrocardiology*, (2011).
3) S. J. Williamson and L. Kaufman: *J. Mag. and Mag. Mat.*, **129**, 129 (1981)
4) R. L. Fagaly: *Review of Scientific Instruments*, **77**, 101101 (2006)
5) Gian Luca Romani, Samuel J. Williamson, and Lloyd Kaufman: *Review of Scientific Instruments*, **53**, 1815 (1982).
6) I. Sasada, and Y. Nakashima: *J. Appl. Phys.*, 103, 07E932 (2008)
7) Y. Nakashima, Y. Suzuki, I. Sasada, M. Shimada, and T. Takeda: *IEEE TRANS. MAG.*, **46**, 2318-2321, (2010).
8) Mahgoub, A.U.; Sasada, I.: *IEEE TRANS. MAG.*, **50**, 1, (2014)
9) A. Mahgoub, Y. Suzuki, M. Nishimura, and I. Sasada: *Electronics, Communications and Computers (JEC-ECC), 2012 Japan-Egypt Conference on,* 200-204, 6-9 Mar 2012
10) I. Sasada: *J. Appl. Phys.*, **91**, 7789 (2002)

Received July. 10, 2016; Revised Aug. 16, 2016; Accepted Sept. 06, 2016